The Virtual Reference Clock (VRC) Time Scale of the NRCan Real Time Wide Area GPS Correction Service (GPS·C)

F. Lahaye, P. Collins and J. Popelar, Natural Resources Canada, Geodetic Survey Division.
francois.lahaye@nrcan.gc.ca

Abstract

Twelve Real Time Active Control Points (RTACPs) distributed across Canada continuously monitor all GPS satellites in view by means of dual frequency high precision geodetic GPS receivers using external atomic frequency standards (active and passive H-Masers, Cs and Rb oscillators). Each RTACP communicates dual-frequency pseudo-range and carrier phase measurements in real-time at 1 Hz to a central computer which generates wide-area GPS corrections with an update rate of 2 seconds. Ionosphere-free, carrier-phase filtered pseudo-range data are combined with ultra-rapid GPS satellite orbit predictions and fixed RTACP coordinates in a least-squares adjustment to determine satellite and station clock offsets with respect to a virtual reference clock (VRC). The VRC is maintained as a weighted mean of adjusted RTACP receiver clocks and is related to a smoothed mean GPS system time derived from the broadcast clock parameters of all tracked satellites. The current VRC algorithm is based on RTACP receiver clock predictability reflecting the stability of the atomic frequency standards involved over both the short and long term. This approach provides a stable system time scale by mitigating the effects of individual RTACP data availability and quality, as well as instabilities of the external frequency standards. The VRC algorithm provided the most stable reference when compared to any single clock in the system for time intervals of up to a few hours. At the same time the VRC effectively eliminated the systems dependence on a single GPS receiver's performance and has not been affected by short data dropouts.

Introduction

In 1996, the Natural Resources Canada's Geodetic Survey Division (GSD) implemented a prototype real-time GPS Correction Service (GPS•C) with the objective to facilitate increased accuracy of real-time GPS positioning within the national geodetic reference frame for the Canadian landmass and adjacent oceans. In support of the GPS•C correction service, majority of the stations in the Canadian Active Control System (CACS) network of dual frequency high precision geodetic GPS receivers was upgraded to facilitate real-time GPS data communication to a central data processing facility to generate wide-area GPS corrections. The original system architecture, the data communication infrastructure and the application software technologies are described in Caissy *et al* [1996]. The positioning performance of the system is reviewed in Skone *et al* [1996] and Lahaye *et al* [1997] and use of the system for remote clock performance monitoring is described in Lahaye *et al* [2001a, 2001b]. Fig. 1 shows the current configuration of the real-time component of the CACS network (RTCACS), which supports the GPS•C service scheduled to production in 2002.

The following sections present the GPS data processing, satellites and stations clock parameter estimation and the VRC time-scale generation performed in real-time at the central computing facility. The reader is referred to Lahaye *et al* [1997] and Lahaye *et al* [1998] for previous descriptions of the system.

General Context and Constraints

It is important to outline the context in which the GPS•C time scale is generated because it imposes constraints on the processing that do not apply in more traditional timing applications. Since the system's sole source of timing information are GPS pseudorange and carrier phase observations obtained in real-time from remote GPS receivers, any clock models derived from these measurements will reflect the behaviour of the GPS receiver clocks as driven by the external frequency standard. Therefore, the GPS data characteristics will impact the clock models and their interpretation has to take it into account. As the primary function of the GPS•C system is the generation of GPS wide area corrections for real-time positioning, the service coverage, i.e. the number of GPS satellites for which corrections are available, must be maximised at all times by accommodating all GPS receiver clocks in the system regardless of

their quality and stability. Due to data communication delays the GPS data from some remote sites may not be available on time resulting in gaps in the observation series thus producing inhomogeneous solutions. Because of these constraints, the GPS data processing and the system time scale generation algorithm is implemented in a time sequential filter, which has to be very robust in detecting bad data and assuring that GPS receiver clock events are properly taken into account.

The GPS•C algorithm used in generating satellite clock corrections is implemented in two steps performed every two seconds (Fig. 2). In the first step all the GPS observables for a given epoch which pass misclosure test are used to generate satellite and receiver clock phase solutions relative to the VRC. This process uses short term clock models to assess the quality of the GPS data, detect possible GPS receiver clock phase discontinuities and determine *a priori* weights for selected clocks for the least-squares estimation. The clock phase solutions are used in the second step to update the short- and long-term clock models in preparation for the next epoch processing. Maintenance of the VRC is achieved through weight assignment to clocks of the system within these two steps. Schematic diagrams of process and data flow for these two processing steps are depicted in Fig. 3 and 4 and are described more fully in the following two sections.

GPS Data Processing

Observation Equations

The pseudorange and carrier-phase data represent the time delay between the GPS signal transmission from the satellite and its detection at the receiver as measured by the difference of the corresponding satellite and receiver clocks. This delay can be expressed as the sum of the geometric satellite range delay, the tropospheric delay, the ionospheric delay, relativistic effects and it also includes the satellite and receiver clock misalignment. In the case of carrier phase, an unknown cycle ambiguity must be added to the observation equation (Eq. 1). In general, the pseudorange measurements show a noise of about 50cm whereas the noise of the carrier-phase data is at a centimetre level if cycle ambiguities can be correctly resolved. Thus

$$
\begin{aligned}
P_{f\,sta}^{\,sat} &= \left(f^{sat} - f_{sta}\right) + \left(r_{sta}^{sat} + d_{sta\,ion}^{sat}(f) + d_{sta\,trop}^{sat} + d^{sat}{}_{rel}\right)/c + e_{P_f} \\
L_{f\,sta}^{\,sat} &= \left(f^{sat} - f_{sta}\right) + \left(r_{sta}^{sat} - d_{sta\,ion}^{sat}(f) + d_{sta\,trop}^{sat} + d^{sat}{}_{rel} + l_f N_{f\,sta}^{\,sat}\right)/c + e_{L_f}
\end{aligned}
\qquad \text{(Eq. 1)}
$$

where

$P_{f\,sta}^{\,sat}\ L_{f\,sta}^{\,sat}\ e_{P_f}\ e_{L_f}$	are pseudorange and phase observations and errors at frequency f ;
$f^{sat}\ f_{sta}$	are satellite and station clock phases;
$r_{sta}^{sat}\ d_{sta\,ion}^{sat}(f)\ d_{sta\,trop}^{sat}\ d^{sat}{}_{rel}$	are geometric, ionospheric and troposphe ric delays and relativistic correction;
$l_f\ N_{f\,sta}^{\,sat}$	are wavelenght and phase ambiguity at frequency f , and
c	is the speed of light.

Data Filtering

At one second intervals, each GPS receiver pseudorange and carrier-phase observations, corrected to the first order for the ionospheric delay by combining the measurements on the L1 and L2 frequencies, are used to compute a weighted average of the differences between the corrected pseudorange and carrier-phase measurements and an integration of the corrected carrier-phase (Eq. 2). At the start of a satellite pass, or when a cycle slip is detected, the averaging and integration are restarted. The weights used are based on the satellite angular elevation above the local horizon at the receiver site. Although the ionosphere-corrected data combinations show increased short-term noise in comparison with the L1 data by a factor of about 3, as the weighted average converges to the ionosphere-free carrier-phase ambiguity, the noise of the filtered pseudoranges decreases to about 5 cm. However, the averaging takes some time to converge, mainly due to the increased pseudorange noise for satellites at low elevation angles. The detection of cycle slips is important and only filtered pseudoranges below a configurable threshold are used in the subsequent processing.

$$
\begin{aligned}
P_{3\,sta}^{sat} &\approx 2.54 \cdot P_{1sta}^{sat} - 1.54 \cdot P_{2sta}^{sat} \\
L_{3sta}^{sat} &\approx 2.54 \cdot L_{1sta}^{sat} - 1.54 \cdot L_{2\,sta}^{sat} \\
w_{sta}^{sat} &= \left(a_o + a_1 \cdot \exp\left(- elv_{sta}^{sat} / elv_0\right)\right)^{-2} \\
\overline{P}_{3\,sta}^{sat}(t_n) = \left(L_{sta3}^{sat}(t_n) - L_{sta}^{sat}(t_0)\right) + \sum_{i=0}^{n} \left(P_{sta\,3}^{sat}(t_i) - L_{sta3}^{sat}(t_i)\right) w_{sta}^{sat}(t_i) / \sum_{i=0}^{n} w_{sta}^{sat}(t_i) = & \\
\left(f^{sat} - f_{sta}\right) + \left(r_{sta}^{sat} + d_{sta\,trop}^{sat} + d^{sat}{}_{rel}\right) / c + e_{\overline{P}_3} &
\end{aligned}
\qquad \text{(Eq. 2)}
$$

where t_n is the current time, t_0 is the filter initialisation time, elv_{sta}^{sat} is the satellite elevation at current time and a_o, a_1 and elv_0 are the weighting function parameters.

Epoch Data Selection and Reduction

The filtered pseudoranges are stored in revolving buffers containing a data history for the twelve most recent epochs from each GPS receiver in the real-time tracking network. An epoch is selected from this data set for processing, using criteria that minimise the correction service latency and maximise its coverage while assuring adequate representation of data from GPS receivers equipped with high quality atomic frequency standards. Also, elevation angle masks can be applied for individual stations and data can be screened based on convergence level of the filtered pseudoranges.

GPS satellite positions are interpolated from predicted ephemerides and the geometric satellite ranges are computed in the observation equations using precise receiver antenna coordinates. Since October 2001, the orbit predictions are obtained every 3 hours from the NRCan ultra-rapid orbit determination process [Tétreault *et al*, 2002]. Before October 2001, the IGS combined ultra-rapid products [Weber *et al*, 2002] were obtained every 12 hours and are now used as an alternate source. Satellite orbit predictions are checked for availability and compared with the broadcast ephemerides. If an orbit prediction is not available or if the difference between the predicted and the broadcast ephemerides exceeds 15m, satellite positions are derived from broadcast ephemerides, until the next orbit predictions are obtained.

The tropospheric delays are computed using the Hopfield model for the corresponding satellite elevation angle and relativistic corrections are based on the dot product of the instantaneous satellite position and velocity as follows:

$$
d^{sat}{}_{rel} = -2\left(\overline{x}_{sat} \cdot \dot{\overline{x}}_{sat}\right) / c \qquad \text{(Eq. 3)}
$$

Finally, *a priori* satellite and GPS receiver clock phases are estimated from short-term clock models in order to compute *a priori* misclosures of observation equations to be used in the least-squares adjustment.

Screening *A Priori* Misclosures

When adequate short-term satellite and GPS receiver clock models are available the average and standard deviation of *a priori* misclosures are computed per satellite and per receivers. When the absolute value of a given average exceeds a configurable threshold by more than about 3 times the associated standard deviation, the corresponding satellite or receiver clock is flagged as a potential clock phase discontinuity and is subsequently estimated without constraints.

Least-Squares Adjustment

The *a priori* misclosures of filtered pseudoranges for the selected epoch are used in a least-squares adjustment to determine corrections to the short-term clock phase predictions. In the adjustment, weights are assigned to the filtered pseudoranges and are proportional to the satellite elevation angles using a formula similar to that introduced in Eq. 2. The least-squares adjustment is constrained according to *a priori* information based on the clock model statistics as described in the next section. When the

screening of the *a priori* misclosures detects a potential clock phase discontinuity, the constraint for the associated clock correction is removed to allow free estimation of the parameter.

When the system of equations is solved for an epoch, residuals are formed and screened for potential bad data using residual testing. The least-squares solution and residuals screening are iterated until no bad data is detected. Then, the *a priori* clock phase predictions are updated with their solved corrections to produce new clock phase solutions for the selected epoch that will be used in clock modelling.

Clock Modelling and VRC Time Scale Generation and Control

Clock Modelling

Time based polynomials of up to degree 3 can be used to model both the receiver and satellite clock phase offsets with respect to the VRC. If t_n denotes the current epoch then

$$\begin{aligned} \Delta t_i &= t_n - t_i \\ f_i = f(t_i) &= a_0 + a_1 \Delta t_i + a_2 \Delta t_i^2 + a_3 \Delta t_i^3 \\ &= \begin{bmatrix} 1 & \Delta t_i & \Delta t_i^2 & \Delta t_i^3 \end{bmatrix} \begin{bmatrix} a_0 \\ a_1 \\ a_2 \\ a_3 \end{bmatrix} \end{aligned} \qquad \text{(Eq. 4)}$$

The clock models parameters are updated in real-time using a sequential least-squares scheme with epoch clock phase solutions weighted as a first order Markov process according to their age and a given correlation time. At the processed epoch t_n, the clock model parameters are derived as in Eq. 5 where T is the correlation time. The actual implementation is sequential and does not require storage of a long history of clock phase solutions.

$$\begin{bmatrix} a_0 \\ a_1 \\ \vdots \\ a_n \end{bmatrix} = \begin{bmatrix} \sum_i w_i & \sum_i w_i \Delta t_i & \cdots & \sum_i w_i \Delta t_i^3 \\ \sum_i w_i \Delta t_i & \sum_i w_i \Delta t_i^2 & \cdots & \sum_i w_i \Delta t_i^4 \\ \vdots & \vdots & \ddots & \vdots \\ \sum_i w_i \Delta t_i^3 & \sum_i w_i \Delta t_i^4 & \cdots & \sum_i w_i \Delta t_i^6 \end{bmatrix}^{-1} \begin{bmatrix} \sum w_i f_i \\ \sum w_i \Delta t_i f_i \\ \vdots \\ \sum w_i \Delta t_i^3 f_i \end{bmatrix} \qquad \text{(Eq. 5)}$$

$$w_i = \exp(-\Delta t_i / T)$$

Two such models are maintained for each of the GPS receiver and satellite clocks to follow their short and long-term variations. First degree polynomials are used for all clocks with typical correlation times of 6 minutes for the short-term and 1 and 2 days for the long-term models. Second degree polynomials with correlation time of 10 seconds were used for the satellites short-term clock models while the Selective Availability (SA) was in effect. The short-term clock models provide *a priori* values of the receiver and satellite clock offsets for the least-squares adjustment.

When the epoch least-squares clock phase solution confirms a clock phase discontinuity, the corresponding model is set to a "learning" mode when the long-term model correlation time is reduced to that of the short-term model. This "learning" mode is maintained for a period of time to assure rapid convergence of the long-term clock model to a new level before the long-term correlation time is restored.

While in "learning" mode and for a configurable additional period of time called the "deweight" mode, the clock is assigned zero weight both in the least-squares solution and in the VRC determination scheme described below.

VRC Implementation

Two basic approaches have been implemented for the determination and maintenance of the GPS•C system reference clock. One is to use one of the GPS receiver clocks in the network as the system reference clock and the other is to derive a Virtual Reference Clock as a weighted mean of selected clocks in the system. The first approach is relatively simple to implement but makes the whole system completely dependent on a single station and its performance, which is highly undesirable from an operational point of view. The second approach requires an efficient way to combine several clocks into a single VRC time scale and deal with sudden changes in individual clock data availability and behaviour. The system can be switched from one to the other scheme via operator intervention.

The VRC time scale of the real-time GPS•C service is determined in two steps. In the first step, the epoch least-squares solution produces corrections to the predicted clock phases using *a priori* weights equal to the inverse of the squared RMS of fit of the short-term models, reflecting the short-term clock model noise levels. A configurable maximum weight can be assigned to each input clock. No constraints are presently applied for the estimation of short-term satellite clock model updates, although the least-squares adjustment implementation allows for it. In the second step, the VRC update correction to the least-squares epoch clock phase solutions is computed as a weighted average of the clock phase updates for selected GPS receivers *a priori* long-term models. The weights are based on the phase separation between the short- and long-term models of individual GPS receiver clock as specified in Eq. 6, with configurable maximum value. Fig. 5 shows examples of both weights, typical for GPS receivers with external H-maser, Cs and Rb oscillators. Clock phase discontinuities due to GPS receiver resets are closely monitored by screening *a priori* misclosures and, when such a reset is detected, the corresponding weights set to zero for the duration of the "learning" period or if the operator invokes so called "deweight" mode.

$$MaxModDif = \max\left(ModDif\left(T_{short}\right), ModDif\left(T_{long}\right)\right)$$
$$ModDif\left(T\right) = \sum_{dt}\left(a_0^{short} - a_0^{long}\right)^2 \exp\left(-\Delta t / T\right) \qquad \text{(Eq. 6)}$$

The VRC is then referred to the mean GPS system clock by differencing the broadcast corrected satellite clocks with the epoch satellite clock phase solutions (Eq. 7) for each observed satellite. These estimates of the phase offset of the VRC with respect to the GPS system time as derived from the broadcast satellite clock parameters are used in a long-term linear clock model with correlation time of 1 to 3 days to smooth variations of the broadcast corrected satellite clocks.

$$f_{GPS}^{sat} - f_{VRC}^{sat} = (t^{sat} - t_{GPS}) - (t^{sat} - t_{VRC}) = (t_{VRC} - t_{GPS}) = f_{GPS}^{VRC} \qquad \text{(Eq. 7)}$$

VRC Initialisation and Operator Control

The VRC is usually initialised by assigning zero weights to all but one GPS receiver clock with an external H-maser frequency standard. This represents the first option toward the realisation of the GPS•C system reference clock as outlined above when the VRC offset and drift with respect to the mean GPS system clock are those of the selected reference GPS receiver clock. The VRC is then aligned with the mean GPS system clock by the operator by making phase and frequency adjustment to all the clock models in the system. The VRC weighting scheme described above is then introduced with appropriate maximum weights for selected GPS receiver clocks to contribute to the maintenance of the VRC. The VRC is then running free as long as it stays within acceptable limits with respect to the broadcast derived GPS system time. When the VRC and GPS time start diverging, the operator can re-align them by making appropriate phase and frequency adjustment to all clocks models in the system. Other operator controls include setting maximum weights and fixing weights for specific clocks, adjusting clock model correlation times, forcing clock "learning" mode, etc.

VRC Stability Assessment

The GPS•C wide area correction service using the VRC algorithm described above is run continuously in real-time since 1996. To demonstrate the VRC performance the states of the systems were sampled and saved at the exact one-minute GPS epochs for the month of July 2001. During the month the system operated automatically with only a single operator intervention to align the VRC to the mean GPS system time on July 11th, 2001. The system configuration was to maximise usage of all GPS tracking data and use 5 RTCACS H-maser equipped stations (ALB2, ALGO, DRAO, NRC1 and USN2) to maintain the VRC. The two other H-masers stations (NRC2 and YELL) and all Cs and Rb clocks were excluded from VRC update computation and freely estimated.

As the short-term GPS receiver clock models RMS of fit shown in Fig. 6 resulted in weights which were much larger than the maximum allowed (1 ns^{-2}), the maximum weights were in effect for the 5 H-maser driven GPS receiver clocks with no constraints on all the remaining clocks in the system. Fig. 7 shows the short- and long-term clock model phase differences as determined from Eq. 6 (MaxModDiff) for the 5 selected GPS receiver clocks. The weight for USN2 was fixed at 1 ns^{-2} while the maximum weights allowed for the 4 other clocks were set at 0.25 ns^{-2}. The actual weights used in the VRC update computation are shown in Fig. 7 and the computed VRC updates in Fig. 8 together with its integration over time. The latter is useful to assess the effectiveness of the algorithm in maintaining the VRC.

The July 11th realignment of the VRC to the mean GPS system time as derived from the broadcast satellite clock parameters is evident in Fig. 9. This alignment estimate reflects the uncertainty of the mean GPS system time determination, which is given by the long-term clock model RMS of fit of about 6 ns.

The Total Allan deviations (TotADev) [Howe, 1999] were derived, using the Tavella and Premoli [1994] method modified by Ekstrom *et al* [1999], for 6 GPS receivers controlled by H-maser (ALGO, DRA2, NRC1, NRC2, USN2, YELL), 2 controlled by Cs (PRDS, STJO) and 2 by Rb (SCH2, WHIT) oscillators, along with the implied VRC. Uninterrupted 20 days of clock phase data after the July 11th alignment were used (Fig. 10) to produce the Total Allan deviation curves in Fig. 11. The VRC provides the best short term stability required by the GPS•C wide area correction service despite of the fact that diurnal GPS receiver clock variations reported in Lahaye *et al* [2001a] affect the VRC stability after few hours. It is expected that the planned implementation of carrier-phase based solution, described in Collins *et al* [2001], will improve the VRC long-term stability significantly.

Conclusion

The implementation of the VRC time scale in the real-time GPS•C wide area correction service has been described. The present system uses ionosphere-free carrier-phase filtered pseudoranges, rapid satellite orbit predictions and fixed tracking network station coordinates in a least-squares estimation to update in 2 second intervals individual satellite and GPS receiver clock phase offsets. These are used to update short and long term polynomial clock models in a weighted sequential stochastic process generating the VRC. The VRC control is achieved by clock phase weight assignment in the least squares estimation, the selection of maximum weights and long term correlation times for clocks contributing to its maintenance and its phase and frequency parameters can be set by the operator as required. The VRC relation to the mean GPS system time is continuously monitored as the smoothed difference between the broadcast corrected and GPS•C determined clocks of all GPS satellites actively tracked at any given time.

As shown by the total Allan deviation graphs for GPS receiver clocks controlled by 6 H-masers, 2 Cs and 2 Rb oscillators over 20 days interval, the VRC provided the most stable reference when compared to any single clock in the system for time intervals of up to few hours. At the same time the VRC effectively eliminated the systems dependence on a single GPS receiver's performance and has not been affected by short data dropouts.

Future work will concentrate on improvements to the least-squares weighting, use of undifferenced ionosphere-free carrier phase data and related improvements of the GPS data reduction model to include, among other things, earth and ocean tides, satellite phase wind-up effects, etc. Moreover, real-time estimation of carrier-phase ambiguities, tropospheric delays and corrections to predicted satellite orbits are being implemented. These changes are expected to increase significantly the timing accuracy and will result in corresponding improvements in clock modelling and the VRC stability.

Acknowledgements
The authors wish to acknowledge the important contributions of their colleagues at the Geodetic Survey Division, the Frequency and Time Group of the Canadian National Research Council, and the US Naval Observatory.

References

Caissy, M., P. Héroux, F. Lahaye, K. MacLeod, J. Popelar, J. Blore, D. Decker, and R. Fong (1996), "*Real-Time GPS Correction Service of the Canadian Active Control System.*", ION GPS 1996, the Proceedings of the 9th International Technical Meeting of the Satellite Division of the Institute of Navigation, Kansas City, Missouri, USA, September 17-20; pp. 1787-1791.
(http://www.geod.nrcan.gc.ca/site/index_e/products_e/publications_e/papers_e/Real-Time_Correction.pdf)

Collins, P., F. Lahaye, J. Kouba and P. Héroux (2001), "*Real-Time WADGPS Corrections from Undifferenced Carrier Phase.*", Proceedings of the National Technical Meeting of the Institute of Navigation, Long Beach, California, USA, January 22-24; pp. 254-260.
(http://www.geod.nrcan.gc.ca/site/index_e/products_e/publications_e/papers_e/real.pdf)

Ekstrom, C. R., F. Torcaso, E. A. Burt and D. N. Matsakis (1999), "*Estimating the stability of N clocks with correlations.*", Joint Meeting of the European Frequency and Time Forum and the IEEE International Frequency Control Symposium, 1999, 168-172.

Howe, D. A. (1999), "*Total Variance Explained.*", Joint Meeting of the European Frequency and Time Forum and the IEEE International Frequency Control Symposium, 1093-1099.

Lahaye, F., P. Collins, P. Héroux, M. Daniels and J. Popelar (2001a), "*Using the Canadian Active Control System (CACS) for Real Time Monitoring of GPS Receiver External Frequency Standards.*", Proceedings of ION GPS 2001, the 14th International Technical Meeting of the Satellite Division of the Institute of Navigation, Salt Lake City, Utah, USA, September 11-14, pp.2220-2229.
(http://www.geod.nrcan.gc.ca/site/index_e/products_e/publications_e/papers_e/ION_GPS2001.pdf)

Lahaye, F., P. Collins, P. Héroux, M. Daniels and J. Popelar (2001b), "*Monitoring GPS Receiver and Satellite Clocks in Real Time: A Network Approach.*", GPS World, Vol. 12 No. 11, November 2001, pp. 44-50.

Lahaye, F., M. Caissy, J. Popelar and R.J. Douglas (1998), "*Real-Time GPS Monitoring of Atomic Frequency Standards in the Canadian Active Control System (CACS).*", Proceedings of the 30th Annual Precise Time and Time Interval (PTTI) Systems and Applications Meeting, Reston, Virginia, USA, December 1-3, pp. 187-198.
(http://www.geod.nrcan.gc.ca/site/index_e/products_e/publications_e/papers_e/1998RealTimeGPS.pdf)

Lahaye, F., M. Caissy, P. Héroux, K. MacLeod and J. Popelar (1997), "*Canadian Active Control System Real-Time GPS Correction Service Performance Review.*", Proceedings of the National Technical Meeting of the Institute of Navigation, Santa Monica, California, USA, January 14-16; pp. 695-699.
(http://www.geod.nrcan.gc.ca/site/index_e/products_e/publications_e/papers_e/Jan97IONGPS_C.pdf)

Skone, S., M.E. Cannon, K. Lochhead, P. Héroux, F. Lahaye (1996), "*Performance Evaluation of the NRCan Wide Area System.*", ION GPS 1996, the Proceedings of the 9th International Technical Meeting of The Satellite Division of the Institute of Navigation, ION GPS-96, Kansas City, Missouri, USA, September 17-20; pp. 1787-1791.
(http://www.geod.nrcan.gc.ca/site/index_e/products_e/publications_e/papers_e/WAS_Evaluation.pdf)

Tavella P. and A. Premoli (1994), "*Estimating the instabilities of N clocks by measuring differences of their readings.*", Metrologia, 30, 479-486.

Tétreault, P., Y. Mireault, B. Donahue, P. Héroux, C. Huot (2002), "*NRCan IGS Analysis Center Report for 2000.*", 2000 Annual Report, Volume II, International GPS Service, IGS Central Bureau at Jet Propulsion Laboratory, Pasadena, CA, USA, to be published.
(http://techinfo.jpl.nasa.gov/igs/files/directory/tetreault_p/tetreault_p.pdf)

Weber, R., T. Springer (2002), "*Analysis A ctivities.*", IGS 2000 Annual Report, Volume I, International GPS Service, IGS Central Bureau at Jet Propulsion Laboratory, Pasadena, CA, USA.
(ftp://igscb.jpl.nasa.gov/igscb/resource/pubs/2000_an_rpt.pdf)

Tables and Figures

Table 1 Status of RTACP external atomic frequency standards during the month of July 2001.

Stations	Freq. Std.
ALB2	Passive HM
ALGO	Active HM
CHUR	Cs
DRA2(DRAO)‡	Passive HM
NRC1† NRC2†	Active HM/AOG Passive HM
PRDS	Cs
RAYM	Off-line
SCH2	Rb
STJO	Cs
USN2	HM/AOG
WHIT	Rb
WINN	Cs
YELL	Active HM

†common antenna reference.
‡common clock reference and antenna.
AOG: auxiliary output generator.

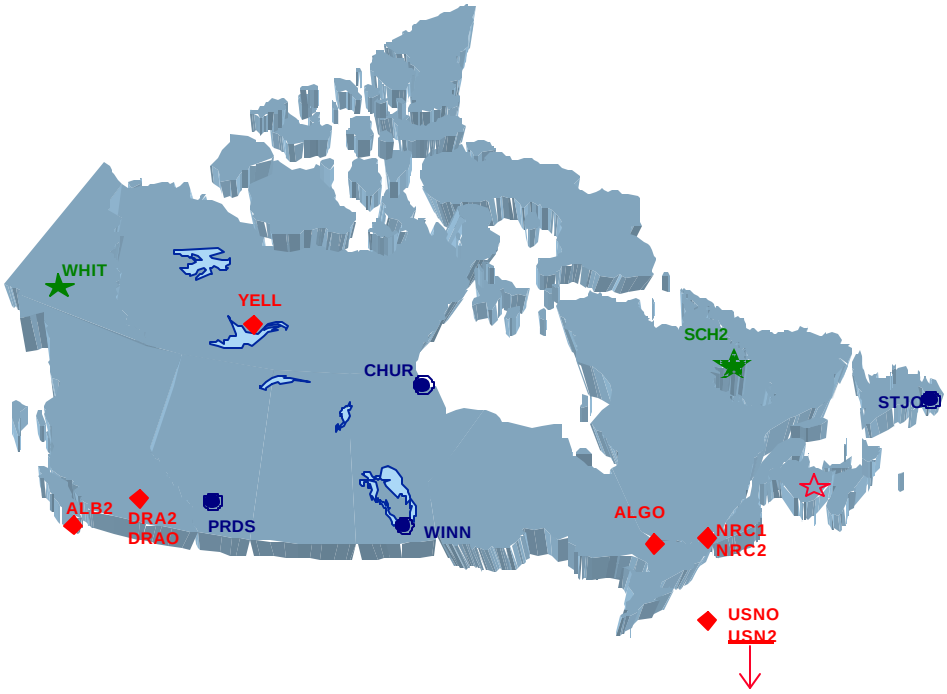

Figure 1 CACS network of real-time automated tracking stations (solid symbols) and a potential new site (open star). Red diamonds designate sites equipped with Hydrogen Masers, blue disks show sites with Cesium and green stars are those with Rubidium frequency standards.

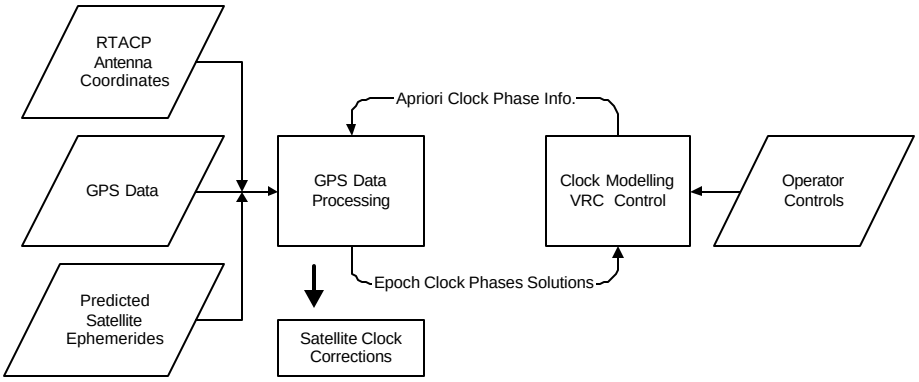

Figure 2 General schematic diagram of the GPS•C processing scheme.

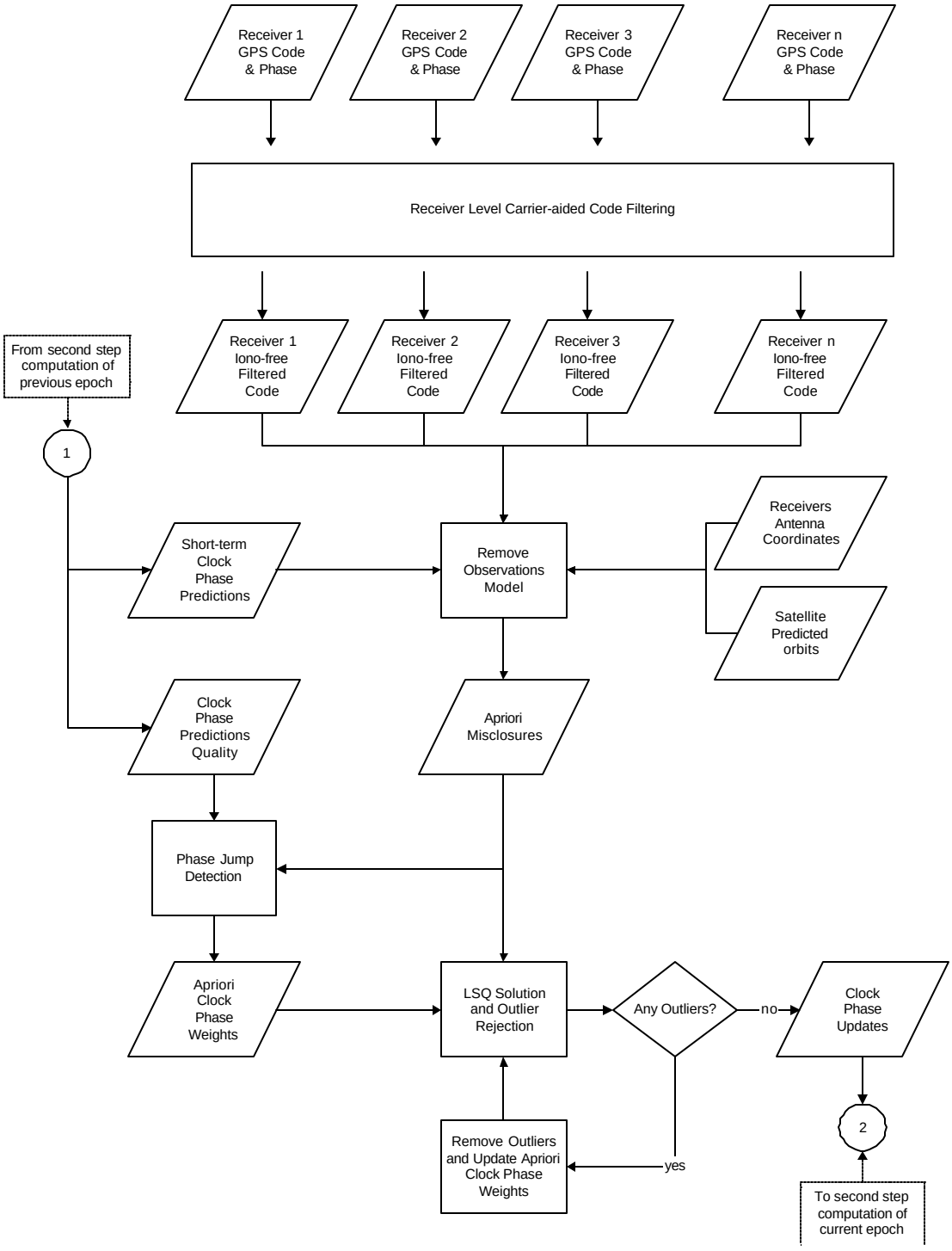

Figure 3 Schematic flow chart of the first step in the real-time GPS•C data processing: epoch GPS data reduction.

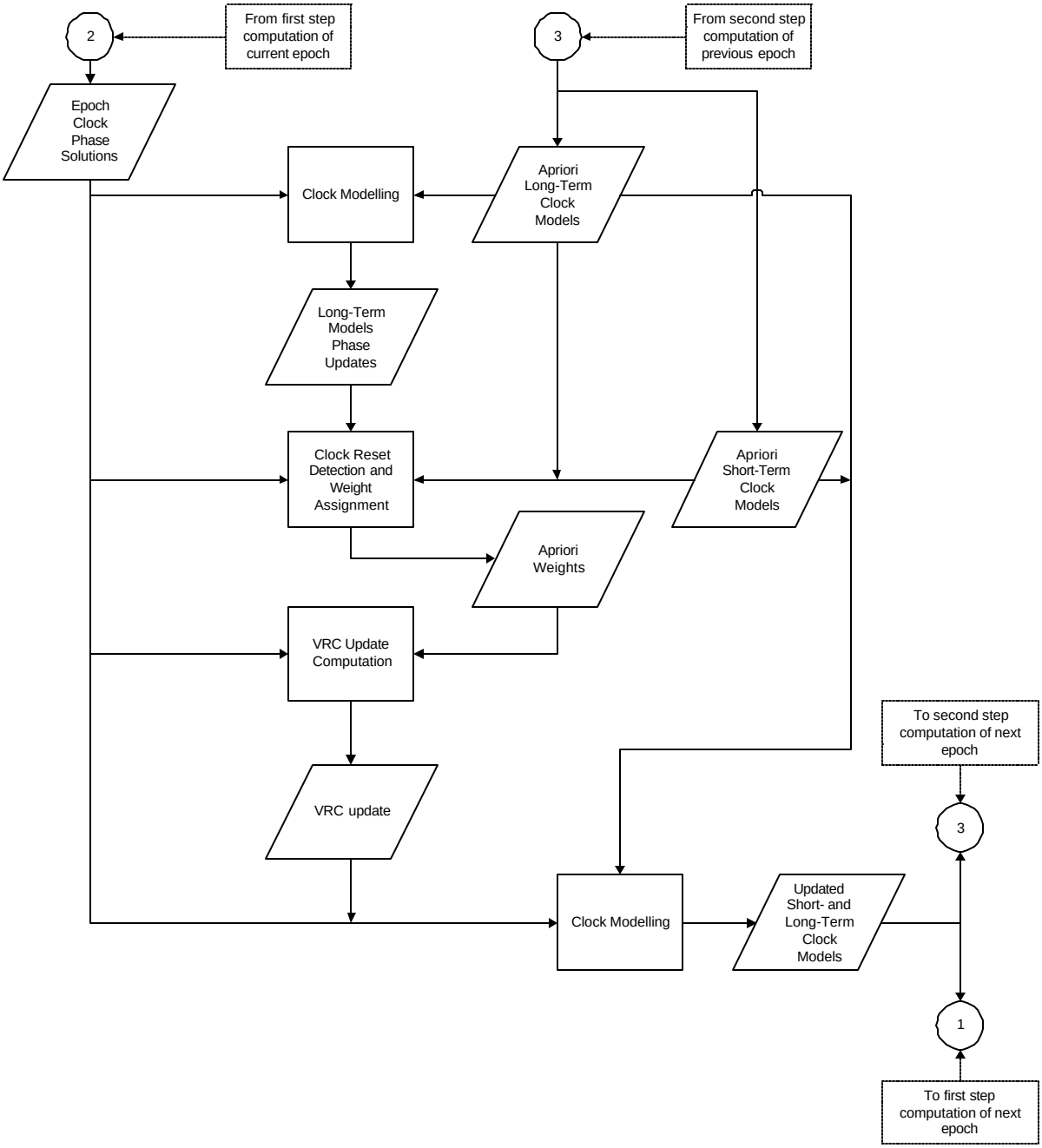

Figure 4 Schematic flow chart of the second step in the real-time GPS•C data processing: clock modelling.

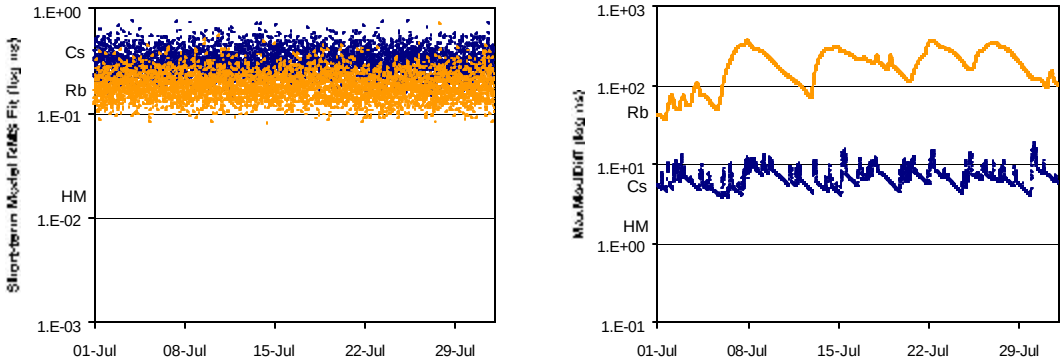

Figure 5 Typical short-term model RMS of fit and values of MaxModDiff for HM, Cs and Rb driven GPS receiver clocks.

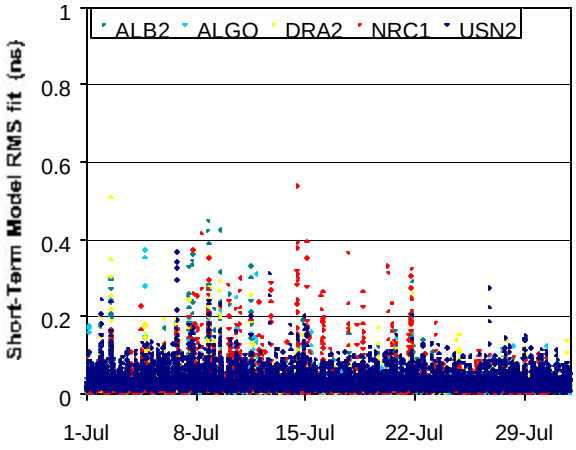

Figure 6 Short-term model RMS of fit for GPS receiver clocks during July 2001.

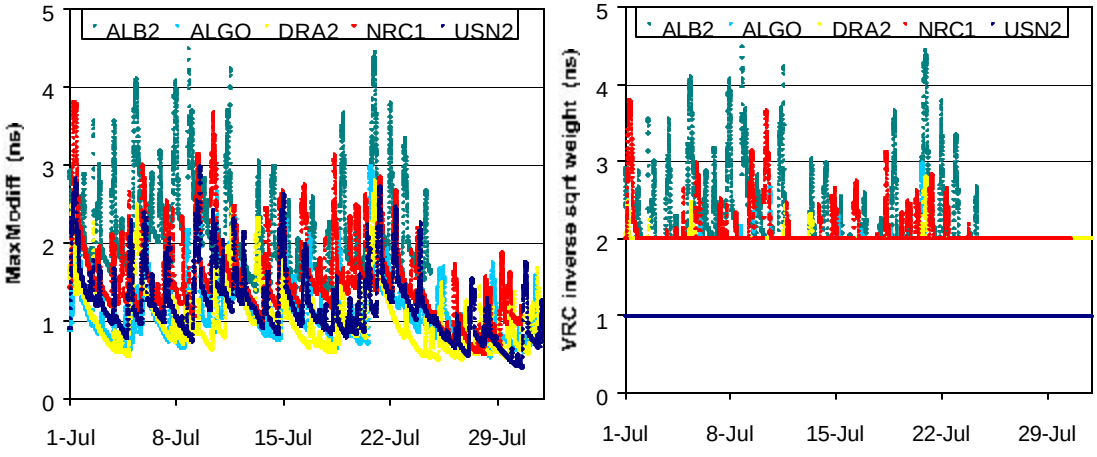

Figure 7 MaxModDiff values and corresponding VRC update weights for GPS receiver clocks during July 2001.

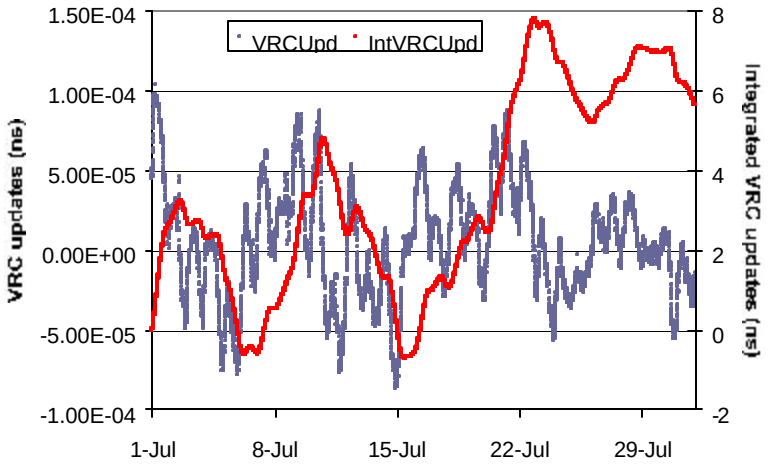

Figure 8 VRC updates and integrated VRC updates during July 2001.

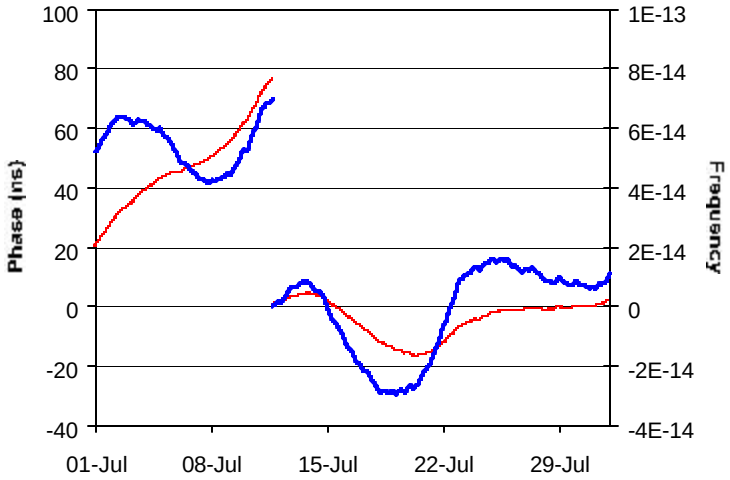

Figure 9 The estimated long-term model parameters of difference between the VRC and the mean GPS system time as determined from the differences between the GPS?C and the broadcast corrected satellite clocks.

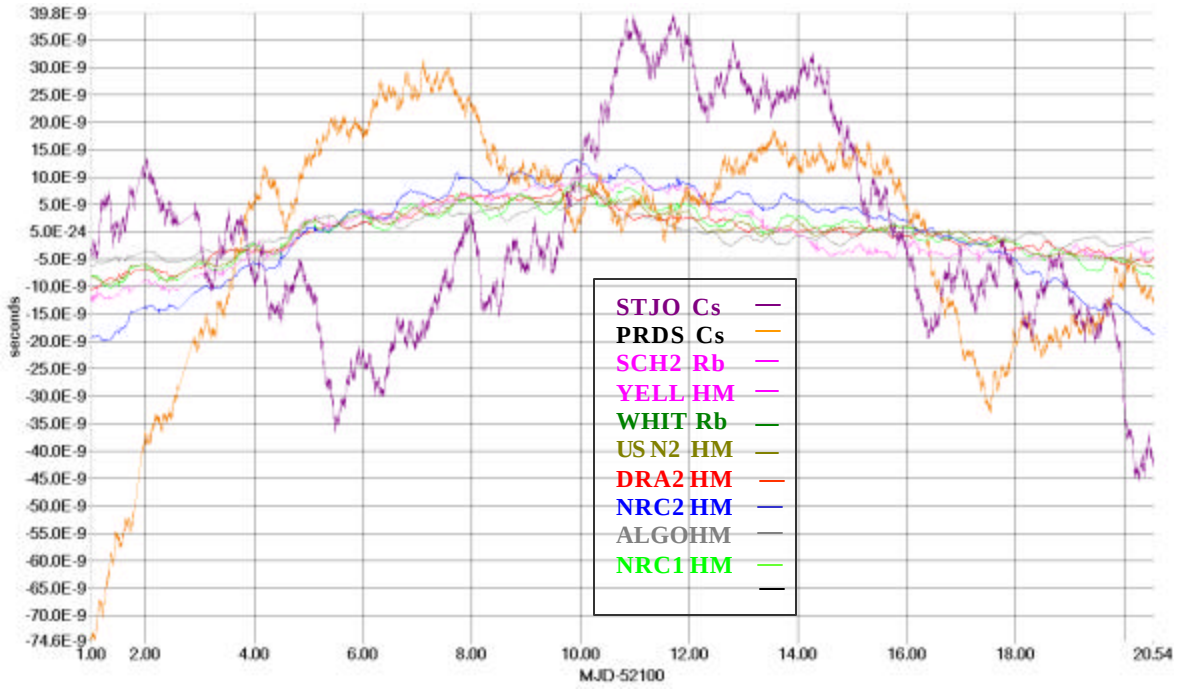

Figure 10 De-trended (mean phase and frequency offset removed) GPS receiver clock phase variations used for computation of the Total Allan deviation shown in Fig. 11 (Rb out of scale).

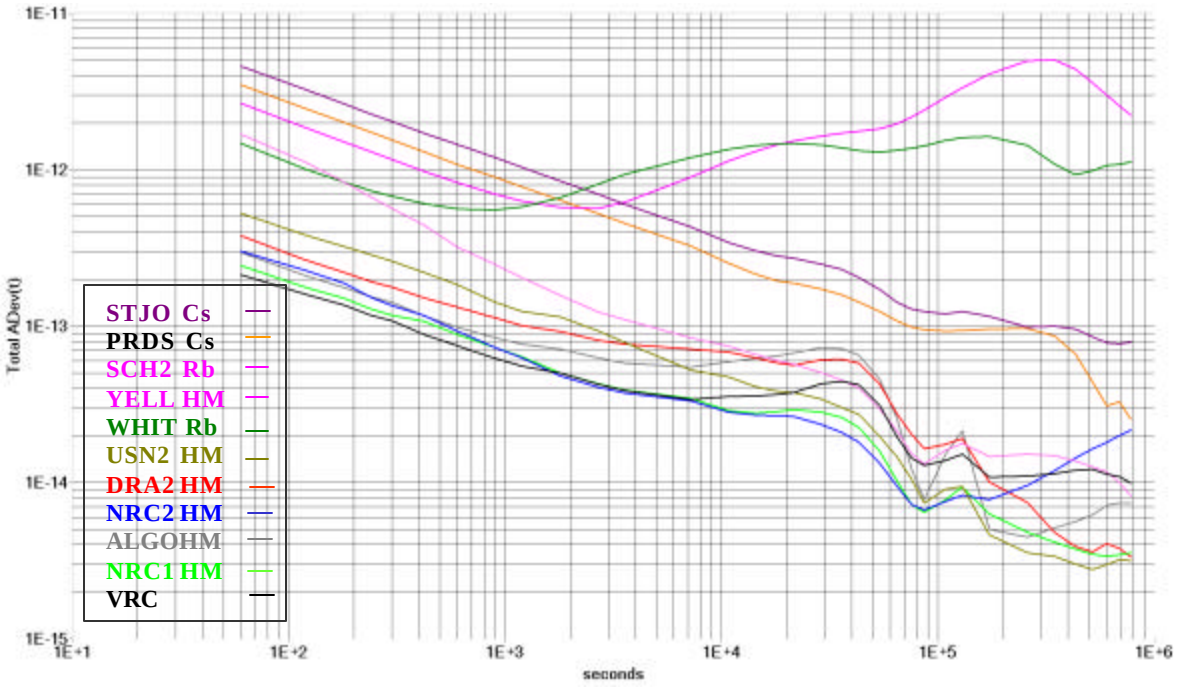

Figure 11 Total Allan deviations computed from de-trended real-time GPS receiver clock phase solutions for the 20 days data set in July 2001.